ELSEVIER

Earth and Planetary Science Letters 200 (2002) 1–14

EPSL

www.elsevier.com/locate/epsl

Constraints on hydrothermal processes on basaltic edifices: inferences on the conditions leading to hydrovolcanic eruptions at Piton de la Fournaise, Réunion Island, Indian Ocean

F.Jh. Fontaine [a,*], M. Rabinowicz [a], J. Boulègue [b], L. Jouniaux [c]

[a] *Laboratoire de Dynamique Terrestre et Planétaire, UMR 5562, 14 Avenue Edouard Belin, 31400 Toulouse, France*
[b] *Laboratoire de Géochimie, Physicochimie et Fluides Géologiques, UPMC, UPRESA 7047, 75252 Paris Cedex 05, France*
[c] *Ecole Normale Supérieure de Paris, Laboratoire de Géologie, UMR 8538, 24 rue Lhomond, 75231 Paris Cedex 05, France*

Received 7 September 2001; received in revised form 25 February 2002; accepted 7 March 2002

Abstract

The hydrothermal processes that occur on the active basaltic edifice of Piton de la Fournaise are investigated. The present-day volcanic activity concentrates in a west–east-oriented collapsed area, 13 km long and 6–8 km large, called Enclos Fouqué. Enclos Fouqué is open to the sea on its eastern side, while a horseshoe rim delimits its extension to the west, south and north. This forms a continuous cliff, 100–200 m high above the floor of Enclos Fouqué. Inside Enclos Fouqué, a 400 m high basaltic cone with two coalescent summit craters constitutes the most active area of the volcano. Beyond the western wall of Enclos Fouqué, a wide basaltic plateau called the Plaine des Sables stretches west for a few kilometers, until it reaches a cliff limiting its western part. To the north and south of this plateau, rivers notch the basaltic edifice, and along the slopes of the induced valleys springs flow. Geochemical data from these springs indicate hydrothermal activity within deep fractured media inside the plateau generated owing to west–east regional extension. On the floor of the Plaine des Sables, near the western wall of Enclos Fouqué, extensive ash deposits from a violent hydrothermal eruption have been recognized. Hydrothermal activity has also been detected in the deep (>100 m) porous layers of Enclos Fouqué, in an area surrounding the central cone. This circulation occurs in layers of vesiculated rocks that constitute a highly permeable and quasi-isotropic medium. Physical models are presented to illustrate the basic differences between the thermal regime of each hydrothermal system. We show that, in the periphery of the volcano, the fracture walls stabilize the hydrothermal circulation inside the fissure network, thus steadily draining the heat along the impermeable walls. Consequently, hot (230–240°C) rising convective currents with a finger shape, 150 m distant, reach the uppermost parts of the fracture. By contrast, inside the isotropic porous layers of the central area, the circulation is likely to be chaotic/turbulent because of the high permeability of the medium. This scatters the thermal energy through the whole porous media. Numerical models of the transient evolution of the hydrothermal circulation in the fractured medium are presented. They reveal that the fingers generated in the deep levels of the edifice move upward at a velocity of 15–150 m/yr, depending on the amplitude of the fracture

* Corresponding author. Tel.: +33-5-6133-2844; Fax: +33-5-6133-2900.
E-mail address: fontaine@pontos.cst.cnes.fr (F.J. Fontaine).

PII: S0012-821X(02)00599-X

permeability. The extensive character of the stresses in the Plaine des Sables, the velocity and the high temperature inside the hydrothermal flow constitute necessary conditions for the disruption of the fracture walls during boiling. Using a model of Germanovich and Lowell [J. Geophys. Res. 100 (1995) 8417–8434], these conditions are shown to be sufficient for the generation of huge (km^3 of deposits) hydrothermal eruptions in the periphery of the edifice, while only small (a few m^3 of deposits) hydrovolcanic events are shown to develop at the summit area. Accordingly, the ash deposits (0.6 km^3) recovered near the western wall of Enclos Fouqué are ascribed to the hydrothermal flow in fractures generated by the east–west extensional stresses.

Keywords: hydrothermal processes; volcanism; models; fractures; Piton de la Fournaise

1. Introduction

Hydrovolcanic phenomena are catastrophic eruptive/explosive events that sometimes accompany volcanic/magmatic activities. These events violently eject a mixture of water, steam and rock particles. According to Smith and McKibbin [2], these phenomena can be classified into two types: phreatomagmatic and steam-blast events. Phreatomagmatic eruptions occur when hot magmatic products contact groundwater or seawater. The erupted deposits contain amounts of fresh glassy magmatic products. Steam-blast events account for eruptions that did not involve the expulsion of juvenile rock. Among these steam-blast type eruptions, Smith and McKibbin [2] itemize: gas eruptions, when the driving fluid is gas or superheated steam, phreatic eruptions, when the driving fluid is groundwater (essentially of meteoric origin), and hydrothermal eruptions, which require a pre-existing hydrothermal system.

To understand the physical mechanisms driving hydrovolcanic events, the choice of a well studied and monitored site is fundamental. We focused our study on the Piton de la Fournaise which is one of the most active and monitored basaltic volcanoes in the world, erupting every 11–18 months [4]. Its build up started at least 500 000 years ago on the eastern flank of the Piton des Neiges (a nearby extinct volcano, Fig. 1) [3]. Thereafter, the volcanic activity moved to the east. Its present location results from three successive collapses separating four phases of magmatic activity [5] (Fig. 1). The youngest collapse, which formed the horseshoe structure called Enclos Fouqué (EF in Figs. 1 and 2), has been dated to 4000 years by analysis of cosmic ray-produced ^{3}He and ^{21}Ne [6]. The present-day volcanic activity (fourth magmatic phase) concentrates inside Enclos Fouqué which is composed of a 400 m high central cone, two diffuse rift zones and two coalescent – Bory (BC in Fig. 1) and Dolomieu (DC in Fig. 1) – summit craters. The magmatic activity is characterized by two preferential orientations for outlets: N10 and N170 (rift zones). A third orientation (N120, thought to be the main tectonic direction) has been evidenced, but is not involved in the present-day activity [5].

At the Piton de la Fournaise, except for a permanent fumarolic vent that has been active since 1986, there is no obvious hint of hydrothermal activity. In fact, the best evidence of hydrothermal activity comes from the geophysical studies of the volcano. It has been established by electric measurements (self-potential (SP) anomalies) that hydrothermal activity takes place in the active central cone. In fact, the positive SP anomalies (up to 2 V) detected inside the cone have been interpreted as convective ascending currents generated by thermal transfers via infiltrated meteoric water (6–10 m/yr) [7,8]. A shallow magmatic complex provides the necessary heat [5,9]. Recently, Lénat et al. [10] confirmed this hypothesis by studying the resistivity structure of the edifice. Indeed, the development of superficial layers (about a few hundred meters under the top of the cone) with low resistivities in the cone is associated to the influence of a coupled hydrothermal/magmatic complex. Nevertheless, little is known about hydrothermal activity that develops inside the cone. Particularly, the evidence of an aquifer has not been established yet.

Some arguments also lead to the hypothesis that hydrothermal activity develops in the periphery of the volcano. The western parts of the volcano are notched by deep valleys where erosion

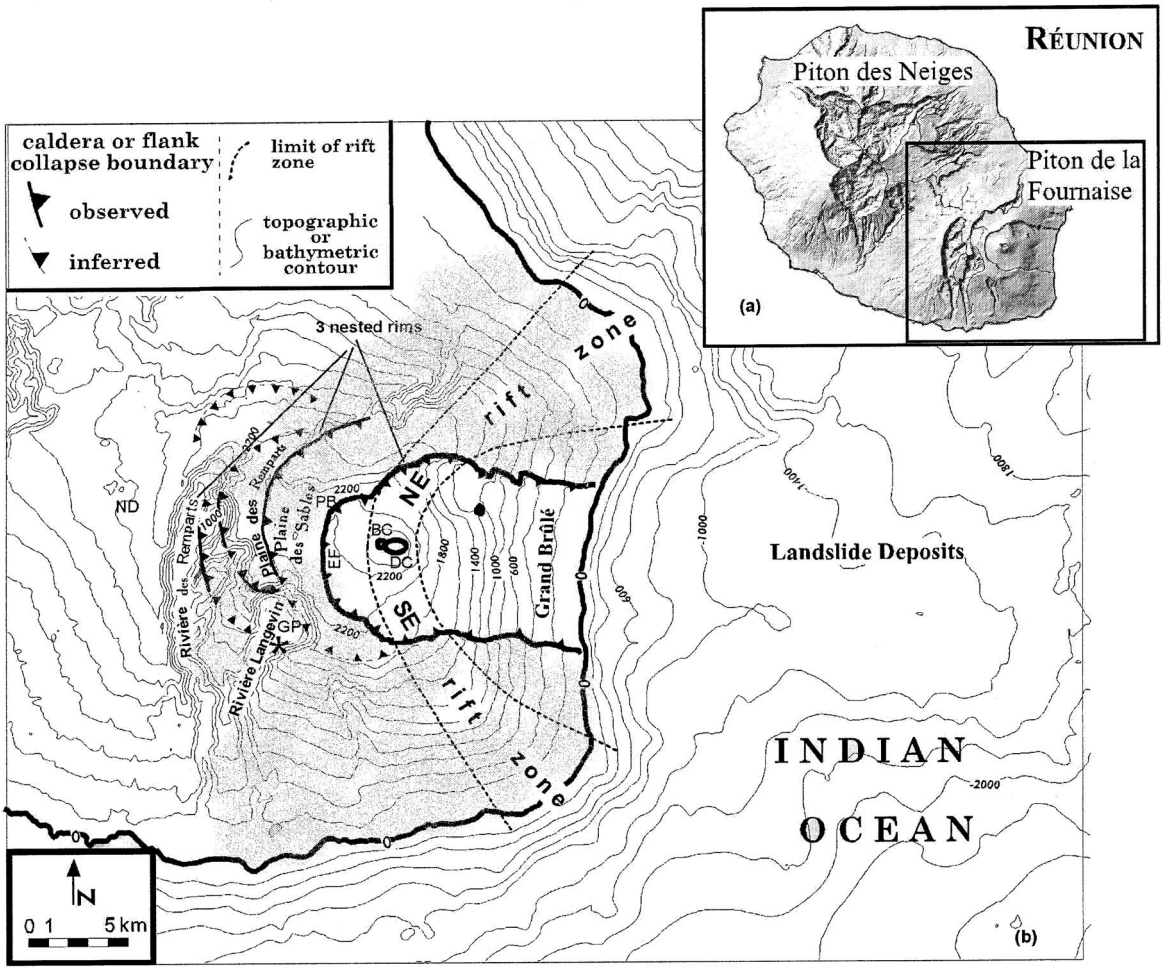

Fig. 1. (a) Réunion Island. (b) Main structures of the edifice of Piton de la Fournaise. EF: Enclos Fouqué; GP: Grand Pays circus; PB: Pas de Bellecombe; ND: Notre Dame area; BC: Bory Crater; DC: Dolomieu Crater; asterisk: location of the spring with anomalous $\delta^{13}C$ and fluor concentration. The gray area corresponds to the extension of the BAM. Also represented: the locations of the main fracture zone, N 10°, N 170° (rift zone northeast and southeast), and the lines of iso-elevation. Modified map after Lénat et al. [10].

digs rivers. The depth of these gorges lies between several hundred and a thousand meters. In the walls of Grand Pays (a collapse area upstream from Rivière Langevin, GP in Fig. 1), hydrothermal minerals have been recovered [11]. The resistivity structure under the Plaine des Sables (see Fig. 1) show the development of a conductive layer (resistivity $\leq 100\ \Omega$ m) at 1 km depth [10]. The interpretation of such conductive layers in the context of the Plaine des Sables is problematic, because it is an inactive area today. It has been inferred that these layers may be representative of a hydrothermally altered zone [10]. Moreover, gravimetric studies underneath the Grand Pays area (Fig. 1) show the settling of a dense intrusive complex, about 1 km below sea level. In fact, the presence of hydrothermal minerals and of a dense intrusive complex combined with the local extension suggests that Grand Pays is a potential area for geothermal exploitations [12]. Recent geochemical investigations by Boulègue et al. [13] show that local anomalies of dissolved fluoride

and sulfate in springs of the eastern walls of Langevin valley are related to the input of hydrothermal related elements in the local aquifers. Locally $\delta^{13}C$ of dissolved carbonates are also typical of input of mantle-related CO_2 in contrast to most other cold springs in Réunion Island [13].

Hydrovolcanic events have been evidenced in the periphery of the volcano as well as along its axis. It has been shown that a particularly violent hydrovolcanic phase – which we called the Bellecombe Hydrovolcanic Events (BHE) – occurred in the periphery of the edifice. The resulting deposits of the BHE, the Bellecombe Ash Member (BAM), are scattered on the floor of the Plaine des Sables (see Fig. 1), near the western wall of Enclos Fouqué (EF in Figs. 1 and 2). The deposits are composed of units of pyroclastic flows and falls of phreatic, phreatomagmatic and hydrothermal origins. Their estimated volume reaches 0.6 km^3. The dating by ^{14}C of a piece of wood embedded in these deposits indicates similar ages for the formation of Enclos Fouqué and for the BHE (about 4000 years), suggesting that the formation of Enclos Fouqué is linked to the BHE [14].

In addition to the BHE, other hydrovolcanic events (mainly phreatomagmatic and phreatic ones) have been evidenced at the summit of the volcano. Important 'historical' phreatomagmatic/phreatic events (for example in 1791 and 1860) have been observed at the top central area, during a period (between 1760 and 1860) when Piton de la Fournaise was in quasi-permanent activity [14]. The conditions leading to such events have been inferred by Bachèlery [5] on the basis of the model of Jaggar and Finch [15]. The emission of a large volume of lava ($10–50\times10^6$ m^3 of lava) drives caldera and collapse formation, and rapid steam generation in response to water contacting hot rocks. These eruptions can be classified as 'mixing eruptions', caused by the mixing of groundwater with hot rocks [2]. The huge intensity of the historical events must be related to the particularly active period of the volcano (the event of 1791 is associated with the initiation of a crater, the Dolomieu Crater). In fact, during an eruptive crisis at Piton de la Fournaise, small hydrovolcanic events are observed at the summit of the volcano, as for instance in February–April 1982 [16].

In this study, we first develop, in Section 2, a consistent physical analysis of hydrothermal activity at Piton de la Fournaise, both in the periphery and along the axis of the edifice. On the basis of

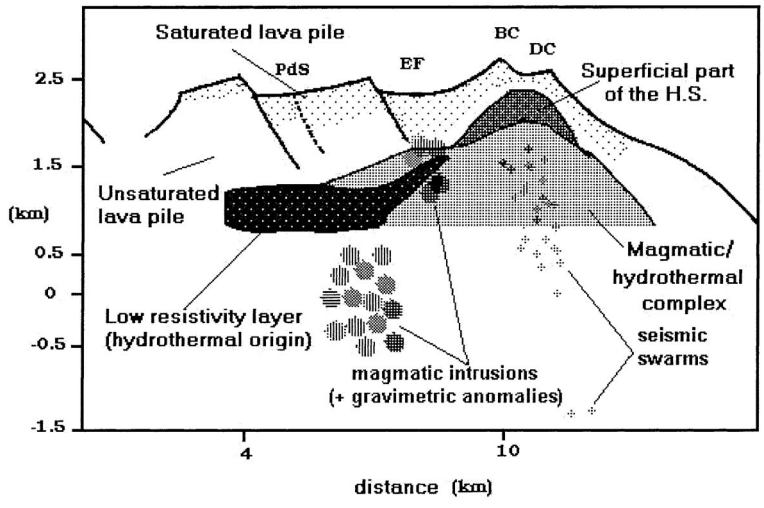

Fig. 2. West–east cross-section of Piton de la Fournaise, from the Plaine des Sables area (PdS) to the central top area, inferred from: resistivity data [10], seismic data [25], gravity data [19], self-potential (SP) data [7,8]. H.S.: hydrothermal system. Note the low-resistivity layer of the top central area, but also the low one of the periphery, beneath the PdS area. Modified cartoon after Lénat et al. [10].

this analysis, we finally (Section 3) discuss the mechanisms leading to hydrovolcanic events.

2. Hydrothermal circulation at the summit and in the periphery of Piton de la Fournaise: physical models

In this section, we show that the axial summit area of the volcano consists in a highly porous medium with a quasi-isotropic permeability field, and that in the periphery, buried layers of dense oceanites are fractured owing to local extension. Then, we present numerical models of hydrothermal convection in a fracture network surrounded by massive basaltic rocks. At the end of this section, we recall the characteristics of hydrothermal circulation in a highly permeable and isotropic porous medium. These models are used to assess the temperature and velocity fields of the hydrothermal flows at the summit and periphery of the volcano.

2.1. Constraints on the permeable media along the axis and in the periphery of the edifice

The eruptive axis constitutes a particular region in a volcanic edifice. The distribution of gas in the magmatic chamber is clearly three-dimensional. The roof of magma chambers being sloped, the volatiles exsolved during the degassing of magma accumulate along the axis of the chamber and ultimately trigger volcanic eruptions [17,18]. Thus, the resulting erupted lavas along the axis are highly vesiculated. The light gravimetric signature of the volcano's axis is consistent with this interpretation [19]. Because of the high concentration of connected voids, highly vesiculated lava is likely to be a highly permeable medium [20]. We measured the permeability of rocks collected at the summit area of Piton de la Fournaise using the apparatus of Jouniaux et al. [21]. The estimated porosity of the samples is about 24% and the permeability 4×10^{-11} m^2. This value is similar to Davis' estimates of the permeability of young porous basaltic lava: about 10^{-10} m^2 [22].

Magmatic overpressures and stresses generate fissures and fractures which enhance the permeability on a larger scale. At Piton de la Fournaise, an intense set of concentric fissures develops around the Dolomieu crater (DC in Fig. 1) and is thought to result from successive inflation and deflation of the structure due to magmatic inputs. An important network of radial fissures develops according to the directions of the rift zones (NE, SE) and to the main tectonic direction N120 (Fig. 1). Accordingly, these two sets of fissures likely increase the permeability inside the cone, but preserve its isotropy. In fact, it has been shown that this fissure network influences SP anomalies. Particularly, maximum positive SP anomalies concentrate where the density of concentric fissures is highest (Bory crater) [7]. The high permeability of the summit area of the Piton de la Fournaise explains that: (i) the meteoric water (6–10 m/yr) rapidly infiltrates the edifice and ii) all attempts to measure magmatic gas flux along the axis have been negative, indicating that the system is highly ventilated. Because gases accumulate along the axis of the magma chamber, gas-depleted magma likely crystallizes in the periphery, promoting the settlement of dense rocks. The positive gravimetric anomalies evidenced by Malengreau et al. [19] in the periphery of the volcano are consistent with the presence of dense, gas-depleted basaltic rocks buried about 1 km deep. Thus, our estimation of the distribution of porosity along the axis and in the periphery of the edifice is compatible with the gravimetric data. The small porosity of the rocks above these intrusions is seen in the lithostratigraphy of the walls of Rivière Langevin (Fig. 1). Particularly, massive oceanites (olivine-rich basalts) produced during the early development of Piton de la Fournaise (500 000 years ago) have been recognized at the base of valley Langevin [5]. At Grand Pays (GP, see Fig. 1), these massive oceanites are fissured and altered by paleo-hydrothermal flows [11]. It is likely that the deep crystallization of rocks occurs with a discontinuous pattern when the magma chamber is dying [19]. Accordingly, the dense bodies recovered on the west side of the volcano likely result from the crystallization of paleo-magma chambers. Rovetta [23] indicates that the permeability of such degassed volcanic rocks is about 10^{-18} m^2. The downward slopes to the north, south, and east

of the volcano induce extension along its western wall (see Figs. 1 and 2). This extensive context triggers a westward fracturing of the edifice [24]. The fissure network kept open by the local tectonics favors the development of a hydrothermal circulation which mines the heat of the magmatic intrusion in the deep levels of the volcano.

To sum up, we suggest the geometry presented in Fig. 2 to describe the internal structure of the edifice from the westward Plaine des Sables area to the central cone (see Fig. 1). The presence of a magma chamber at sea level is inferred from the seismic data of Nercessian et al. [25].

2.2. Hydrothermal activity in the fracture media of the periphery of the volcano

The conceptual model presently developed has already been applied to describe hydrothermalism at mid-oceanic ridge [26,27], and also at continental rift zones [28]. The mathematical and numerical models have been extensively tested, and their full development can be found in previous publications from our group [26,27,29]. Using these codes, we now describe a conceptual model of the fracture, shedding light on the resulting hydrothermal activity.

2.2.1. Conceptual model

The fracture consists of a network of fissures parallel to the fault axis. Typically, the width of the fracture is about several tens of meters. The fissure connectivity along the fault can reach several kilometers and the network vertical extent a few kilometers. In fact, this depends on the nature of the fracturing and thus, on the local tectonics. The local extension keeps the fissures open, permitting fluid percolation. The fracture is surrounded by massive quasi-impermeable walls with a permeability of about 10^{-18} m^2 [23]. The result is that the heat in the walls essentially flows by conduction. We set 380°C as the temperature at the base of the fracture. This temperature corresponds to the demixion temperature of a slightly salted fluid. Let us note that it is the temperature and salinity in the fluid inclusions found in the hydrothermal minerals of the BAM [14]. At the temperature of demixion, two phases coexist: a brine and a fresher component. Because of its buoyancy, the fresh water moves above the critical interface and mixes the meteoric water. Thus, the deep horizon, below the interface, is filled with the brine. The tension at the interface between the fresh water and the brine stratifies convection on both sides of this interface [27]. Accordingly, the bottom of the convective layer of fresh water corresponds to a deep horizon inside the fracture but not to its bottom. At the top of the fracture two situations are possible, open or closed. Closed top conditions are reached if mineral diagenesis seals the system and/or if the fracture does not cross the whole height of the dense complex. This situation can result from an extensive context in the deep levels of the volcano coexisting with a compressive one at a higher elevation. When the hydrothermal circulation emerges in a porous aquifer, the top of the system is considered to be open. This last situation can be compared to the hydrothermal activity at the ridge crest below the pillow lava layer. The data from Piton de la Fournaise cannot aid the decision whether a given hydrothermal system is open or closed. Each of these two situations will be considered in this section. For the model with an open top, the fluid enters the fault at a temperature of 10°C and exits with a zero vertical temperature gradient ($\partial T/\partial z = 0$). For closed conditions, the temperature at the top is 10°C and no fluid flow crosses that interface.

A random perturbation to the initial conductive temperature regime triggers hydrothermal convection inside the permeable network. The heat transported by the flow is mined in the underlying hot rock. Such mining cools the deep layers on time scales of several Ma, i.e. much longer than the lifetime of the hydrothermal system (see below) [26]. The seismic data along the axis of the volcano show that the top of the magma chamber lies 2–2.5 km below the surface [25] (see Fig. 2). It indicates that the conductive gradient does not exceed 0.5°C/m. Thus, a temperature of 380°C is possible at a depth between 700 and 800 m. When the pressure is lithostatic, the fluid does not boil at that temperature and depth. Thus, the fluid circulation should be monophasic at the initiation of the hydrothermal activity. In the equations of convection given by Fontaine et al. [27], the fluid

density (ρ_f) is pressure- and temperature-dependent while the viscosity (μ_f) only depends on the temperature. Accordingly, μ_f varies by a factor of 15 and ρ_f by more than 45%, for the range of temperature and pressure. Fig. 3 shows the geometry of the model (fracture+wall) adopted. In this model, the permeable network consists of a set of parallel fissures confined in a 'porous slot'. Each fissure is separated from the next by a massive quasi-impermeable wall (permeability $k_f = 10^{-18}$ m^2, and thickness $f = 1$ m). For symmetry reasons, the computed box is the half space of Fig. 3. The half fracture thickness ($d/2$) is about 15 m, and the half width of the system is 500 m. The height (H) of the whole system is 500 m, and its length (L) is 500 m. Springs which are known to be in contact with the hydrothermal system emerge from the wall of Rivière Langevin at an elevation of about 1600–1700 m, i.e. about 500 m below the floor of Enclos Fouqué. Hence, a value of 500 m for H is a minimum.

2.2.2. *Permeability amplitude and dynamical benchmarks*

Inside the fracture, the width of the fissure and their spacing are fundamental with regard to the permeability and porosity amplitude. The porosity is defined as: $\varepsilon = \delta/f$ and the permeability as: $k_f = \delta^3/12f$ where δ is the fissure aperture. Typically, for an aperture of about 0.1 mm and spacing of 1 m, the fracture permeability k_f is about 10^{-13} m^2 and the porosity ε is 10^{-4}. These values jump to 10^{-10} m^2 and 10^{-3}, respectively, for an aperture of 1 mm.

The fracture permeability k_f is a parameter whose amplitude is often difficult to assess. At Piton de la Fournaise, little is known about the permeability structure of the edifice. Particularly, the structure of the deep fracture system remains completely unknown. The study of marine hydrothermal systems has led to a few permeability measurements and estimations of the ridge crust. It seems that permeability amplitudes between 6×10^{-13} m^2 and 6×10^{-12} m^2 are lower bound values to generate vigorous hydrothermal activity such as those responsible for hot vents [30]. Such permeabilities are characteristic of fractures in the sheeted dike complex, which is a good analog of the fractured media in the periphery of the volcano because of the extensive context.

Inside the fracture, the permeability in the orthogonal direction is negligible because the wall permeability between two successive fissures is several orders of magnitude lower than the fracture permeability [27]. Consequently, the circulation is almost two-dimensional and confined in the vertical (xz) planes. Such sub-millimeter to millimeter apertures also allow thermal equilibrium to be reached between the fluid and the rock. Thus, fluid and solid temperatures are locally the same in the fault.

The vigor of the convection inside the fault de-

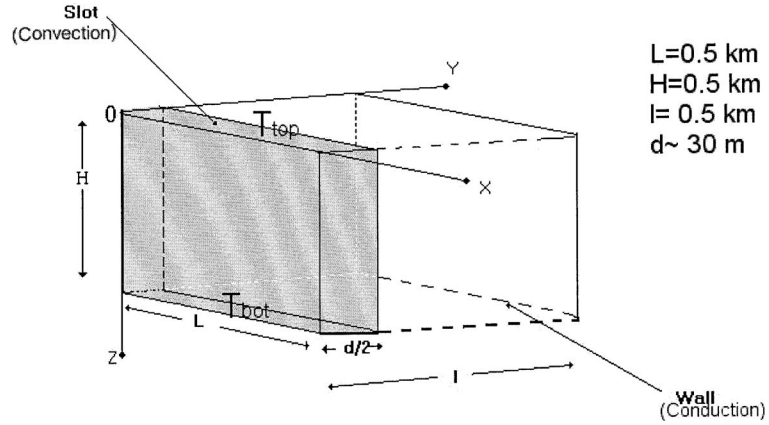

Fig. 3. Geometry of the half space modeled ($y \geq 0$). The flow and temperature fields are symmetrical on both sides of the $y = 0$ plane. $T_{top} = 10$°C, $T_{bot} = 380$°C.

pends on the non-dimensional Rayleigh number (Ra). Ra is defined as:

$$\mathrm{Ra} = \frac{\Delta\rho_f g k_f H}{\mu_0 k} \quad (1)$$

where μ_0 is the viscosity of the fluid at 380°C ($\mu_0 = 7.3\times10^{-5}$ Pa s), g is the gravitational acceleration ($g = 10$ m/s^2), H is the height ($H = 500$ m), κ is the thermal diffusivity of the basalt ($\kappa = 10^{-6}$ m^2/s, and $\Delta\rho_f = 440$ kg/m^3 is the drop in fluid density between 10°C and 380°C. Assuming a permeability range of 10^{-13} m^2 to 10^{-10} m^2, Ra ranges from 3×10^3 to 3×10^6, respectively. Because of numerical limitations, we are only able to run cases at the low end of this range of Ra.

We initiate convective circulation inside the fault by perturbing an initial conductive profile with a small random noise. Then, we iteratively resolve the temperature and flow fields inside the computing box (Fig. 3). Accordingly, we are able to follow the thermal and flow fields of the system with time.

2.2.3. Physical properties

In Fig. 4, we show two models giving the evolution of the hydrothermal flow during its first 20 years for an open and a closed top system. The Ra number of the experiments is 16 000, which corresponds to a fracture permeability k_f of 5×10^{-13} m^2.

Convection develops as fingers, i.e. the convective cells have a small aspect ratio. This is typical of convective processes in fractures thermally influenced by conductive impermeable walls [26]. The characteristic width of the fingers is about 70–80 m, and depends on the amplitude of Ra [26]. In both experiments, the bottom boundary layer is unsteady and thermal instabilities are initiated inside the layer. As seen in Fig. 4, these instabilities are lately collected by the ascending hot plumes. For the open top system, there is no boundary layer at the top of the system, and exit temperature reaches 240°C (0.65) (Fig. 4). For closed top conditions, the top thermal boundary is very thin (15–20 m, i.e. 3–4% of the whole height) and isotherms up to 230°C (0.6) reach the uppermost parts of the fault (Fig. 4). The transient snapshots (Fig. 4a–c) show that the hot thermal front travels from the bottom to the top of the fault in about 15–20 years, i.e. at a velocity of 10–15 m/yr. In fact, modeling shows that this velocity increases linearly with Ra [27]. This means that for $\mathrm{Ra} = 1.6\times10^5$, i.e. for a fracture permeability of 5×10^{-12} m^2, the hot front circulates at a velocity of about 100–150 m/yr. It has been shown that the thermal structure – and particularly the dimensionless asymptotic maximum exit temperature of 0.65 found for open systems – is independent of Ra, d, L and time t [26]. Fig. 4 shows that the convective process is much more developed along the axis of the fault than near the wall. This results from the horizontal thermal gradient across the fault. The convective circulation perturbs the conductive thermal field inside the walls on a distance less than 15 m (see Fig. 4d).

Finally, the mean amount of the heat flowing through the fracture is calculated by adding the mean value of the conductive flow at the top horizontal plane($\lambda^*\partial T/\partial z$, where λ^* is the conductivity of the porous medium in J m/s and T is the temperature in °C) to the advective one ($\rho_f c_f VT$, where $\rho_f c_f$ is the volumetric heat capacity of the fluid in J/m^3 and V the fluid velocity in m/s). After 20 years the heat flowing through the top interface stabilizes around 1.8×10^5 W. It corresponds to a mean of 12 W/m^2 flowing through the 500 m long, 30 m large top of the fracture. This heat is mainly transported by the three rising hot fingers seen in Fig. 4. Thus the power of one finger is less than 10^5 W and corresponds to a 100°C spring with a flow rate of about 0.1–0.2 l/s. 10^5 W is at least two orders of magnitude lower than the heat transported by oceanic vents [31]. As said before, the convective process inside the fault perturbs the conductive profile inside the walls on a distance less than 15 m. Accordingly, the heat anomaly due to a hot finger affects a surface of only 70×70 m^2. Such a heat anomaly is not easy to detect along the western part of the volcano because of the cold fluid circulation in the perched aquifers.

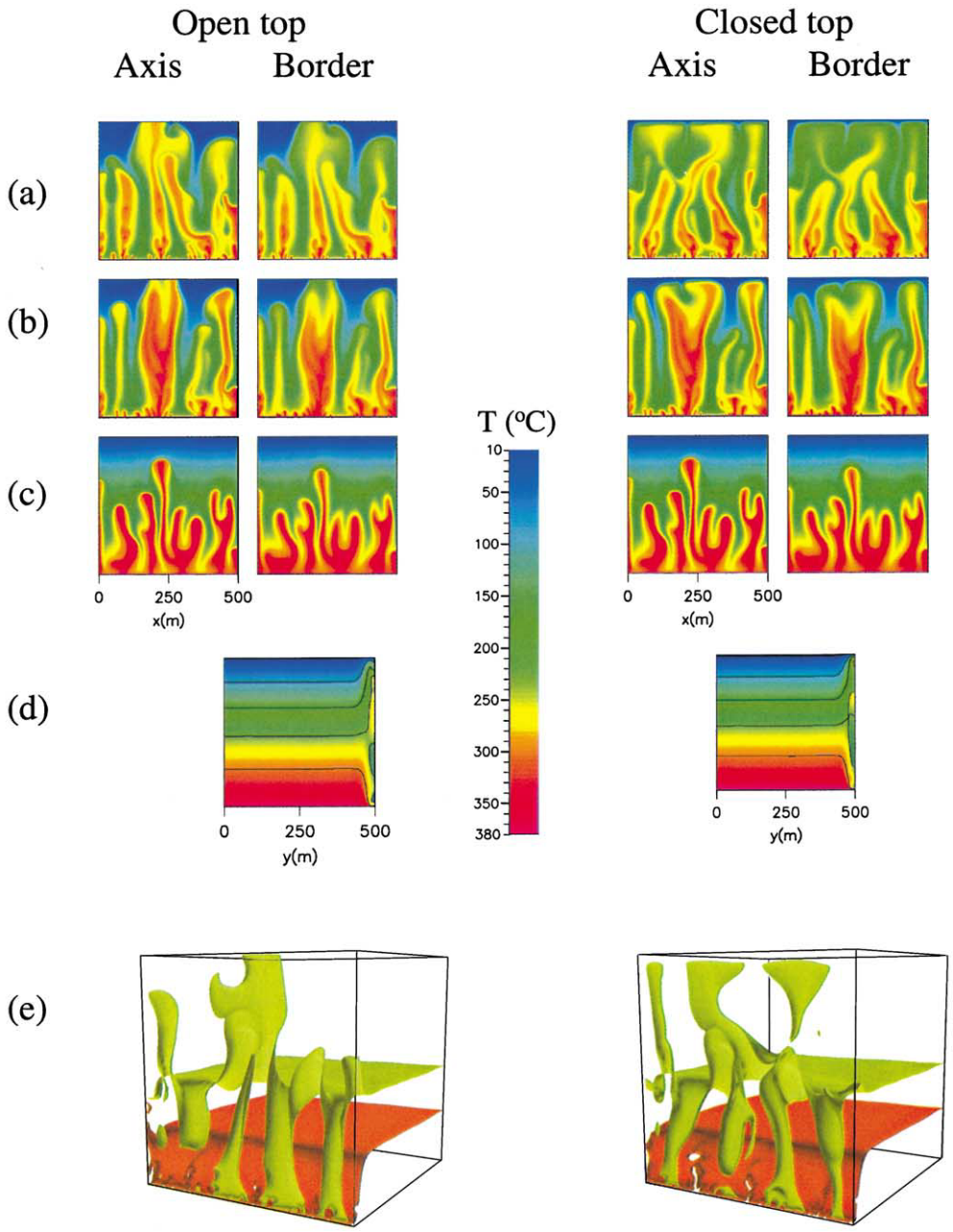

Fig. 4. Thermal characteristics of the hydrothermal flow for open/closed top systems. The Rayleigh number is 16 000 ($k_f = 5 \times 10^{-13}$ m^2). The number of grid points in the x, y and z directions is: 256×64 (5 in the half-fracture, and 59 in the conductive wall) $\times 256$, respectively. Panels a, b and c represent three snapshots of the thermal fields along the axis and border of the fault (xz planes) at time t: (a) $t = 20$ years, (b) $t = 11$ years, (c) $t = 4$ years. Panels d show the thermal field in a cross-section (yz plane) at $x = 250$ m and $t = 20$ years. The temperature drops 74°C between two successive isolines. In panels e we also represent the location of the 240°C (light green) and 305°C (light red) three-dimensional isotherms inside the fault and the wall at $t = 20$ years.

2.3. Some inferences about hydrothermal activity at the summit of the volcano

We have seen that the hydrothermal flows along the axis of the edifice develop in a highly porous medium with a quasi-isotropic permeability of about 10^{-10} m^2. The Rayleigh number Ra associated with this circulation ranges between 10^6 and 10^7. Although this range in Ra number is the same as that of the fractured system, the resulting physical regime is dramatically different. Numerical studies of convective processes in isotropic porous media at such a high Ra number are clearly beyond today's computer possibilities. It has been shown that the circulation exhibits a chaotic/turbulent regime beyond a Ra of 1200–1500 [32,33]. Hence, when $Ra = 10^7$, the hydrothermal convection along the axis of the volcano is likely to be highly turbulent. The Nusselt number Nu (the ratio between convective/conductive heat transfer) increases roughly linearly with Ra ($Nu \propto Ra^e$, with $e \in (0.8,1.3)$) [32]. The result is that the thickness of the thermal boundary layers decreases roughly linearly with increasing Ra. If we consider that this relationship still holds at Ra up to 10^7, the hydrothermal system at the summit of the volcano has a few centimeters thick thermal boundary layer. As observed in numerical experiments of convection in fluids [34], a highly turbulent flow leads to the formation of some time/space-chaotic 'wispy tendrils'.

Also, hydrothermal systems perched in the edifice are likely to be biphasic. Studies of geothermal two-phase systems are numerous (see [35] for a review). Two types of two-phase systems can be distinguished: the majority is liquid-dominated and generates geysers or boiling hot springs; vapor-dominated systems are a minority and display fumaroles and acid springs. Some authors have developed numerical simulations of both types of two-phase systems [36]. However, the modeling of two-phase circulation in a porous medium with an isotropic permeability field and a Rayleigh number between 10^6 and 10^7 is impossible. Moreover, as said before, at Piton de la Fournaise, natural manifestations of the hydrothermal circulation such as hot springs or fumaroles are weak (only one diffuse fumarolic activity initiated in 1986). We propose that this is related to the airy character of the porous medium at the summit of the volcano.

To sum up, we see in this section that hydrothermalism of two types is likely to affect the edifice of the Piton de la Fournaise: the first one in a fractured, dense complex in the periphery of the volcano, and the second one in the porous layers of the top central area which constitutes a quasi-isotropic highly permeable medium. The thermal structure of both systems is basically different. In the fractured medium, the heat is drained along the walls of the fracture and fluids with asymptotic temperatures as high as 230–240°C reach the top of the fault. By contrast, the chaotic/turbulent two-phase circulation triggered in the porous layers of the central area leads to the formation of very thin thermal boundaries, and ascending currents swamp in the highly ventilated porous medium.

3. Discussion: hydrothermal eruptions at Piton de la Fournaise

The actual basic mechanisms of hydrothermal eruptions are not well known. Nevertheless, a recent model of Germanovich and Lowell [1] of the mechanisms of phreatic eruptions has pointed out some concepts that may be relevant to the mechanisms of hydrothermal eruptions. Their model is based on the crucial assumption that the medium where the fluid circulates has a 'two-scale' permeability: a main permeable crack network and a subsidiary one composed of a sub-network of micro-cracks, isolated cracks and dead-end cracks, which does not significantly contribute to the bulk permeability of the medium. A quantitative analysis shows that the amplitude of the main permeability must be greater than 10^{-12} m^2 and that of the subsidiary one about 10^{-18} m^2. The injection of a dike at shallow depth inside this saturated porous medium drives water to boil and superheated steam circulates inside the main permeable network. The upward transport of steam contributes to heat the rock above and on the sides of the intrusion. This flow generates a hot thermal wave, moving upward at a velocity of

a few hundred meters per year, for a main permeability of 10^{-12} m^2. The heat transported by the wave is transferred to the fluid trapped inside the micro-cracks of the subsidiary network. Upon heating, the fluid-filled cracks of the low permeability medium are pressurized because of the thermal expansion of the fluid, and the cracks start to propagate according to the thermo-elastic stresses. Sufficient heating drives the fluid to boil inside the micro-cracks because of the pressure drop resulting from the volume increase of the cracks. Accordingly, the micro-cracks are filled with a mixture of water and steam and the *PT* conditions lie on the Clapeyron curve. The expanded fluid or steam in the micro-cracks migrates via the subsidiary permeability toward the main one. This leads to a relaxation of the elastic stresses generated because of the fluid expansion and boiling. With a subsidiary permeability of 10^{-18} m^2, the elastic stresses achieve relaxation in 1 year. According to Germanovich and Lowell [1], when the hot wave reaches the surface, the elastic stresses generated inside the rock lead to the failure of the rock in small pieces that can be projected upward. Thereafter, the front of failure propagates inward, down to the depth where the elastic stresses have already been relaxed. The model shows that the height of the excavated zone is directly related to the upward velocity of the hot front. Thus, the velocity of the ascending thermal wave being about a few hundred meters per year (for a main permeability of 10^{-12} m^2), and the relaxation time about 1 year, the excavated height of the crater likely reaches a few hundred meters. Germanovich and Lowell [1] show that the failure process is inhibited when the rock strength exceeds 10 MPa. Rock strengths have been shown to range between 7 MPa and 300 MPa, for sandstones and gabbros respectively [37]. Accordingly, the failure of gabbro can only be considered when extensional tectonic stresses overcome the essential part of the rock strength.

This model can explain the occurrence of the small hydrovolcanic events which occurred at the summit of Piton de la Fournaise [16]. The mean width of the dikes that inject at Piton de la Fournaise is about 1 m [38], and some recent volcanic activities have been attributed to the injection of dikes [39,40]. Ancient dike injections of degassed basalt that do not reach the surface and thus crystallize below the surface can create a local zone of low permeability, embedded in the porous basalts of permeability 10^{-10}–10^{-9} m^2 characteristic of the summit of the edifice. It is known that the eastern part of the central cone gradually moves to the sea at a rate of 20 cm/yr (between 1984 and 1989) because of the repeated injection of dikes in the rift zones (Fig. 1) [41], indicating that the rift zone is partly or wholly under extension. The model shows that the diameter of the crater resulting from such a hydrovolcanic eruption triggered by the intrusion of a 1 m thick dike is 2–6 m [1]. Accordingly, only small hydrovolcanic eruptions are expected at the summit of Piton de la Fournaise.

In fact, the model of Germanovich and Lowell [1] also applies to hydrothermal eruptions triggered by hydrothermal circulation in a fracture. As said before, the key assumption of the model is the presence of a medium with a 'two-scale' permeability: a main one where fluids transport the heat from the heat source and a subsidiary one where thermally expanding fluids in micro-cracks circulate. Clearly, the fracture geometry shown in Fig. 3 is consistent with this two-scale permeability: the set of interconnected fissures being responsible for the main permeability (with amplitude ranging between 10^{-13} and10^{-10} m^2 depending on the width of the fissures), and the meter thick quasi-impermeable walls of permeability of 10^{-18} m^2 (which separate one fissure from another) for the subsidiary network. Moreover, the extension that prevails inside the fracture is likely to favor the development of a hydrothermal eruption triggered by the mechanisms described by the model [1]. Our models of hydrothermal circulation in such a medium with a fracture permeability of 5×10^{-13} m^2 show that the convective circulation is able to drive hot fluids upward ('fingers'), at a temperature up to 230–240°C.

In our models, we see that hot fingers of temperature about 230–240°C reach the top of the fracture. Provided that the fluid pressure there is not too high (less than 20–30 MPa), boiling will occur. The permeability of the subsidiary network

of the fracture being 10^{-18} m^2, according to Germanovich and Lowell [1], the relaxation of elastic stresses occurs in 1 year. We have seen that, for fracture permeabilities of 5×10^{-13} m^2 and 5×10^{-12} m^2, the hot front moves upward at about 10–15 m/yr and 100–150 m/yr, respectively. Thus, the depth of craters can reach 15–20 m for $k_f = 5\times10^{-13}$ m^2 and 150–200 m for $k_f = 5\times10^{-12}$ m^2. The occurrence of craters deeper than 200 m is unlikely, because the hydrostatic pressure at these depths is very close to the boiling pressure of a 230–240°C fluid. It is noteworthy that these last values for a fracture permeability of 5×10^{-12} m^2 are consistent with that of the model of Germanovich and Lowell [1] for the same main permeability. This is due to the fact that their porous flow model is very close to that developed in this study. The initiation of the Enclos Fouqué formation [6] has been shown to be synchronous with the development of the BHE [14], i.e. about 4000 years ago. It is thus likely that it is the BHE, and particularly the hydrothermal eruption (phase 2), that triggered the development of the western rim bordering Enclos Fouqué.

The fracture network through emplaced dense rocks must be initiated owing to the extensional stresses generated by the eastern slopes of the edifice. Then, the fissures propagate toward the surface. The development of hydrothermal circulation inside the fracture leads to the formation of hot rising fingers, distant of about 150 m (Fig. 4). When a hot finger reaches the surface, a 150–200 m deep crater is generated. The time needed for the fingers to reach the surface is short (about 15 years for $k_f = 5\times10^{-13}$ m^2), if not very short (about 1 year for 5×10^{-12} m^2). This forms a series of craters following the plane of fracture forming a horseshoe rim on the western part of the edifice (Fig. 1). The series of craters, 150–200 m deep, distant of about 150 m, is likely to form a 200 m deep, discontinuous notch in the constitutive layers forming the ancient western slopes of Piton de la Fournaise 4000 years ago. Lithostratigraphic units with plastic rheology such as scories level favor landslides due to the destabilized eastern slopes of the volcano and the western notch. These landslides promote the separation of the eastern and western parts of the fracture zone, which initiates the formation of the depression of Enclos Fouqué. The hypothesis we propose for the sequence of events leading to the formation of Enclos Fouqué remains to be tested by specific field arguments. The development of fracturing in the rims of the craters could be tested. This needs extensive observations and sampling on the vertical wall of Enclos Fouqué.

4. Conclusion

With the help of the set of data collected on Piton de la Fournaise, we found that two types of hydrothermal processes develop inside the edifice. The first one, largely evidenced by electric and magnetic surveys, sets along the axis of the volcano, in the top central area. The lava that built up the central cone of Piton de la Fournaise is likely to constitute a porous medium, with a high, quasi-isotropic permeability up to 10^{-10} m^2. Recent geochemical data show that the second type of hydrothermal activity develops in the periphery of the volcano (4–5 km while moving to the west from the central cone). We infer that the extension that results from the destabilized eastern flank that is open to the sea opens pathways to convective fluid circulation by fracturing the dense medium that has crystallized in the periphery of the volcano. We show that fracture permeability ranges between 10^{-13} m^2 and 10^{-10} m^2, while the intrinsic permeability of the dense rock is about 10^{-18} m^2.

Numerical models emphasize the basic differences between the thermal fields of each type of hydrothermal activity. For the system along the axis of the volcano, chaotic/turbulent circulation leads to thermal energy scattering through the whole porous medium and to the formation of very thin eddies (as observed in turbulence in fluids). The fracture medium is modeled as a porous vertical slot that contains a fissure network. The fissures are separated from each other by a meter thick wall of permeability of about 10^{-18} m^2. The models show that, in the fracture medium, the heat is drained along the impermeable walls and hot fluids of temperature up to 240°C (fingers) reach the uppermost parts of the fracture.

With the model for phreatic eruptions developed by Germanovich and Lowell [1], we constrain the hydrovolcanic events that set at Piton de la Fournaise. This model is based on the fact that the medium where fluids circulate has a 'two-scale' permeability: a main one, composed of interconnecting fissures, and a subsidiary one, composed of a sub-network of fluid-filled micro-cracks that does not significantly contribute to the bulk permeability of the medium. The model shows that explosive/eruptive conditions can be reached when the fluid of the subsidiary network starts to boil leading to micro-crack pressurization. Because of: (1) the extensional stresses and (2) the overpressures due to boiling, the country rock can fail, initiating the hydrothermal eruption.

With this model, we show that only small phreatic/phreatomagmatic eruptions, responsible for crater formation of about 2–6 m in diameter, can develop at the summit of the volcano. We also show that the permeability structure of a fracture in the periphery of the central active area – i.e. the main permeable network of fissures that leads to fracture permeability between 10^{-13} m^2 and 10^{-10} m^2, and the subsidiary one of the separating walls of permeability 10^{-18} m^2 – is consistent with that of the model of Germanovich and Lowell [1]. Accordingly, we show that deep cratering is possible in the periphery of the volcano: crater depth can reach 150–200 m with fracture permeability of 10^{-12} m^2.

We relate such mechanisms to a huge hydrothermal eruption (more than 0.5 km^3 of ejected products) that set at the Piton de la Fournaise 4000 years ago. We link this catastrophic event to the initiation of the depression called Enclos Fouqué, which occurred at a similar age. Particularly, the western rim of Enclos Fouqué may be directly linked to the excavation of a series of 150–200 m deep craters. To this, we add that the discovery of older (30 000–20 000 years ago) deposits from possibly hydrothermal eruptions, 7–8 km from Enclos Fouqué while moving to the west, indicates that these catastrophic events may be recurrent through time, founding the hypothesis of future catastrophic events of the same type.

Acknowledgements

This work has been funded by the ECODEV, ACI CATNAT and INSU-Risques Naturels No. 309 programs. The computations were supported by the Centre National d'Etudes Spatiales (CNES). We wish to thank Dr. Michèle Allouche for English improvements, Philippe Labazuy and an anonymous reviewer for their constructive comments.*[AC]*

References

[1] L.N. Germanovich, R.P. Lowell, The mechanism of phreatic eruptions, J. Geophys. Res. 100 (1995) 8417–8434.
[2] T.A. Smith, R. McKibbin, Modelling of hydrothermal eruptions: a review, in: Proc. 19th NZ Geothermal Workshop, 1997, pp. 123–128.
[3] P.Y. Gillot, P. Nativel, Eruptive history of Piton de la Fournaise volcano, Réunion Island, Indian Ocean, J. Volcanol. Geotherm. Res. 36 (1989) 53–65.
[4] J. Dubois, J.L. Cheminee, Application d'une analyse fractale à l'étude des cycles éruptifs du Piton de la Fournaise (La Réunion): modèle d'une poussière de Cantor, C.R. Acad. Sci. 307 (1988) 1723–1729.
[5] P. Bachèlery, Le Piton de la Fournaise (Ile de la Réunion), Etude volcanologique, structurale et pétrologique, PhD thesis, 1981, 230 pp.
[6] T. Staudacher, C.J. Allègre, Age of the second caldera of the Piton de la Fournaise volcano (Réunion) determined by cosmic ray produced ^{3}He and ^{21}Ne, Earth Planet. Sci. Lett. 119 (1993) 395–404.
[7] B. Malengreau, J.-F. Lénat, A. Bonneville, Cartographie et surveillance temporelle des anomalies de polarisation spontanée (PS) sur le Piton de la Fournaise, Bull. Soc. Géol. Fr. 165 (1994) 221–232.
[8] S. Michel, J. Zlotnicki, Self-potential and magnetic surveying of La Fournaise Volcano (Réunion Island): Correlations with faulting, fluid circulation, and eruption, J. Geophys. Res. 103 (1998) 17845–17858.
[9] H. Bureau, F. Pineau, N. Metrich, M. Semet, M. Javoy, A melt and fluid inckusion study of the gas phase at Piton de la Fournaise volcano (Réunion Island), Chem. Geol. 147 (1998) 115–130.
[10] J.-F. Lénat, D. Fitterman, D.B. Jackson, P. Labazuy, Geoelectrical structure of the central zone of Piton de la Fournaise volcano (Réunion), Bull. Volcanol. 62 (2000) 75–89.
[11] J.-P. Ran con, Mise en évidence de 'diapirs' hydrothermaux: example des laves zéolitisées de la phase I du Piton de la Fournaise dans le cirque de Grand Pays, in: Evaluation du potentiel géothermique de l'Ile de la Réunion, Rapport Géologique, BRGM, 1981, pp. 135–137.

[12] A. Gérard, J.-P. Ran con, V. Barthes, Etude détaillée du site de Grand Pays, in: Evaluation du potentiel géothermique de l'Ile de la Réunion, BRGM, 1981, pp. 6–15.
[13] J. Boulègue et al., Fluids in Piton de la Fournaise: volatiles and volcanic activity, in: Report CEE-EVOP, Brussels, 1994, 42 pp.
[14] A. Mohamed-Abchir, Les cendres de Bellecombe: un évènement explosif majeur dans le passé récent du Piton de la Fournaise, Ile de la Réunion, PhD Thesis, 1996, 242 pp.
[15] T.A. Jaggar, R.V. Finch, The explosive eruption of Kilauea in Hawaii 1924, Am. J. Sci. 8 (1924) 353–374.
[16] P. Bachèlery, P.A. Blum, J.L. Cheminée, L. Chevallier, R. Gaulon, N. Girardin, C. Jaupart, F.X. Lalanne, J.L. Le Mouel, J.C. Ruegg, P.M. Vincent, Eruption at le Piton de la Fournaise volcano on 3th February 1981, Nature 297 (1982) 395–397.
[17] C. Jaupart, S. Vergniolle, The generation and collapse of a foam layer at the roof of a basaltic magma chamber, J. Fluid Mech. 203 (1988) 347–380.
[18] S. Vergniolle, C. Jaupart, Dynamics of degassing at Kilauea volcano, Hawaii, J. Geophys. Res. 95 (1990) 2793–2809.
[19] B. Malengreau, J.-F. Lénat, J.-L. Froger, Structure of Réunion Island (Indian Ocean) inferred from the interpretation of gravity anomalies, J. Volcanol. Geotherm. Res. 88 (1999) 131–146.
[20] J. Coudray, P. Mairine, E. Nicolini, J.-M. Clerc, Approche hydrogéologique du Piton de la Fournaise, in: J.F. Lénat (Ed.), Le Volcanisme de La Réunion, Monography, Centre de Recherches Volcanologiques, Clermont-Ferrand, 1990, pp. 307–355.
[21] L. Jouniaux, M.-L. Bernard, M. Zamora, J.-P. Pozzi, Streaming potential in volcanic rocks from Mount Pelée, J. Geophys. Res. 105 (2000) 8391–8401.
[22] S.N. Davis, Change in porosity and permeability of basalt with geologic time, in: Int. Symp. on Hydrology of Volcanic Rocks. UNESCO, Lanzarote, 1974.
[23] M.R. Rovetta, A similarity model of incremental fracture growth in submarine hydrothermal systems, J. Geophys. Res. 98 (1993) 4173–4182.
[24] L.L. Lavier, W.R. Buck, A.N.B. Poliakov, Factors controlling normal fault offset in an ideal brittle layer, J. Geophys. Res. 105 (2000) 23431–23442.
[25] A. Nercessian, A. Hirn, J.-C. Lépine, M. Sapin, Internal structure of Piton de la Fournaise volcano from seismic wave propagation and earthquake distribution, J. Volcanol. Geotherm. Res. 70 (1996) 123–143.
[26] M. Rabinowicz, J.-C. Sempéré, P. Genthon, Thermal convection in a vertical permeable slot: Implications for hydrothermal circulation along mid-ocean ridges, J. Geophys. Res. 104 (1999) 29275–29292.
[27] F.Jh. Fontaine, M. Rabinowicz, J. Boulègue, Permeability changes due to mineral diagenesis in fractured crust: Implications for hydrothermal circulation at mid-ocean ridges, Earth Planet. Sci. Lett. 184 (2001) 407–425.
[28] C. Tournier, P. Genthon, M. Rabinowicz, The onset of natural convection in vertical fault planes consequences for the thermal regime in crystalline basements and for heat recovery experiments, Geophys. J. Int. 140 (2000) 500–508.
[29] M. Rabinowicz, J. Boulègue, P. Genthon, Two- and three-dimensional modeling of hydrothermal convection in the sedimented Middle Valley segment, Juan de Fuca Ridge, J. Geophys. Res. 103 (1998) 24045–24066.
[30] A.T. Fisher, Permeability within basaltic oceanic crust, Rev. Geophys. 36 (1998) 143–182.
[31] M.K. Tivey, Modeling chimney growth and associated fluid flow at seafloor hydrothermal vent sites, in: S.E. Humphris et al. (Eds.), Seafloor Hydrothermal System: Physical, Chemical, Biological and Geological Interactions within Submarine Hydrothermal Systems, Geophys. Monogr. Ser. 91, AGU, Washington, DC, 1995, pp. 158–177.
[32] A.S.M. Cherkaoui, W.S.D. Wilcock, Characteristics of high Rayleigh number two-dimensional convection in an open-top porous layer heated from below, J. Fluid Mech. 394 (1999) 241–260.
[33] J.P. Caltagirone, P. Fabrie, Natural convection in porous media at high Rayleigh number, I, Darcy's model, Eur. J. Mech. B Fluids 8 (1989) 207–227.
[34] D.A. Yuen, U. Hansen, W. Zhao, A.P. Vincent, A.V. Malevsky, Hard turbulent thermal convection and thermal evolution of the mantle, J. Geophys. Res. Planets 98 (1993) 5355–5373.
[35] R.P. Lowell, Modeling continental and submarine hydrothermal systems, Rev. Geophys. 29 (1991) 457–476.
[36] S.E. Ingebritsen, M.L. Sorey, Vapor-dominated zones within hydrothermal systems; evolution and natural state, J. Geophys. Res. 93 (1988) 13635–13655.
[37] B.K. Atkinson, P.G. Meredith, Experimental fracture mechanims data for rocks and minerals, in: B.K. Atkinson (Ed.), Fracture Mechanics of Rocks, Academic Press, San Diego, CA, 1987, pp. 477–525.
[38] L. Stieltjes, D. Robert, Analyse structurale de l'ile de la Réunion: ses implications géologiques et géothermiques, in: Evaluation du potentiel géothermique de l'Ile de la Réunion, Rapport Géologique, BRGM, 1981, pp. 47–93.
[39] V. Cayol, F.H. Cornet, Three-dimensional modeling of the 1983–1984 eruption at Piton de la Fournaise Volcano, Réunion Island, J. Geophys. Res. 103 (1998) 18025–18037.
[40] F. Sigmundsson, P. Durand, D. Massonet, Opening of an eruptive fissure and seaward displacement et Piton de la Fournaise volcano measured by RADARSAT satellite radar interferometry, Geophys. Res. Let. 26 (1999) 533–536.
[41] J.F. Lénat, P. Bachèlery, Structure et fonctionnement de la zone centrale du Piton de la Fournaise, in: J.F. Lénat (Ed.), Le Volcanisme de La Réunion, Monograph, Centre de Recherches Volcanologiques, Clermont-Ferrand, 1990, pp. 43–74.